Nonlocal homogenization of $\mathcal{PT}$-symmetric multilayered structures

Denis V. Novitsky,[1,2,*] Alexander S. Shalin,[2,3] and Andrey Novitsky[4,†]
[1]*B. I. Stepanov Institute of Physics, National Academy of Sciences of Belarus, Nezavisimosti Avenue 68, 220072 Minsk, Belarus*
[2]*ITMO University, Kronverksky Prospekt 49, 197101 St. Petersburg, Russia*
[3]*Ulyanovsk State University, Lev Tolstoy Street 42, 432017 Ulyanovsk, Russia*
[4]*Department of Theoretical Physics and Astrophysics, Belarusian State University, Nezavisimosti Avenue 4, 220030 Minsk, Belarus*

(Received 9 November 2018; published 11 April 2019)

Unique and highly tunable optical properties of $\mathcal{PT}$-symmetric systems and metamaterials enable a plenty of entirely new linear and nonlinear optical phenomena with numerous applications, e.g., for designing subdiffraction lenses, nonreciprocal devices, etc. Therefore, the artificial media with the $\mathcal{PT}$ symmetry attract ever-increasing attention and are now a subject for intensive investigations. One of the commonly used methods providing information about the optical response of artificial nanostructural media is a so-called effective medium theory. Here we examine the possibility of utilizing the effective medium theory for a comprehensive analysis of $\mathcal{PT}$-symmetric multilayered systems composed of alternating loss and gain slabs. We show that applicability of local effective material parameters (or Maxwell Garnett approximation) is very limited and cannot be exploited for a prediction of exceptional points marking a $\mathcal{PT}$ symmetry breaking. On the other hand, nonlocal bianisotropic effective medium parameters can be reliably used, if the thickness of a unit cell is much smaller than the radiation wavelength. In the case of obliquely incident plane waves, we reveal the limitation on the loss-gain coefficient, which should not be too large compared with the real part of the permittivity. We believe that our findings can improve the fundamental understanding of physics behind $\mathcal{PT}$-symmetric systems and advance the development of auxiliary tools for analyzing their peculiar optical response.

DOI: 10.1103/PhysRevA.99.043812

I. INTRODUCTION

$\mathcal{PT}$ symmetry entered physics as a realization of the non-Hermitian quantum mechanics keeping eigenvalues real [1,2]. It soon turned out that the properties of $\mathcal{PT}$-symmetric systems can be relatively easily proved in practice in the optical [3,4] and microwave [5] domains (see also the recent review articles [6,7]). Generally, a $\mathcal{PT}$-symmetric optical system is a periodic structure with balanced loss and gain (the same value of loss and gain coefficients): the field of the eigenmodes is equally distributed between the loss and gain components. When the loss-gain coefficient increases, the balance may spontaneously disappear at the point of symmetry breaking (exceptional point), where the eigenstates become degenerate. In the non-$\mathcal{PT}$-symmetric regime, the field is asymmetrically distributed between the loss and gain parts of the system producing amplifying and decaying eigenmodes. The system may return to the $\mathcal{PT}$-symmetric state at the following exceptional point (see, e.g., Ref. [8]).

Optical $\mathcal{PT}$ symmetry is the basic concept for various prospective applications including lasing [9,10] and coherent perfect absorption [11,12], enhanced sensing [13–15], effects of asymmetric light propagation such as unidirectional invisibility [16], nonreciprocity [17], localization [18], and others. Optical $\mathcal{PT}$-symmetric systems have usually either a waveguide or multilayer configuration, although there are more exotic variants, such as metasurfaces [19,20] or graphene-based structures [21]. $\mathcal{PT}$ waveguides can be described in the coupled-mode approximation and can be both active [22] and passive [23]. The multilayer structure as an important system to understand basics of the PT symmetry without using any approximations will be analyzed in this paper.

A multilayer can be considered as a photonic crystal or a simplest metamaterial (artificial periodic subwavelength structure) [24–26] depending on the relation between the size of the unit cell and the radiation wavelength. A key problem of the metamaterial theory is a homogenization that allows us to treat the metamaterial as a quasicontinuous medium with a set of effective parameters, such as dielectric permittivity and magnetic permeability. Metamaterials of the multilayer geometry can be homogenized using the standard techniques, such as first-principle homogenization [27,28], nonlocal effective-medium theory [29–31], Whitney interpolation [32], etc. However, to the best of our knowledge, there has been no thorough investigation of the homogenization of $\mathcal{PT}$-symmetric systems. In the most relevant article [33], the $\mathcal{PT}$-symmetric system is composed of the hyperbolic metamaterial and gain medium, the former being described using the Maxwell Garnett approach. Although the accurate transfer-matrix solution is available for multilayered systems, it is instructive to have a homogenized solution too. It may not only simplify the description, but also unveil novel regularities. For example, in Ref. [31] the nonlocal homogenization is used to derive the criterion of the effective medium theory breakdown. In Ref. [34] the nonlocal homogenization theory is exploited to prove that the Maxwell Garnett approach is more applicable for the unit cells with inversion symmetry compared to the unit cells without it.

*dvnovitsky@gmail.com
†andreyvnovitsky@gmail.com

In this paper, we employ the operator effective medium approximation (OEMA) [29,31] to investigate its area of validity in description of $\mathcal{PT}$-symmetric multilayered systems. OEMA juxtaposes a homogeneous nonlocal bianisotropic effective medium to the multilayer, thus allowing us to accurately find the transmission and reflection spectra [31] and surface-wave propagation [34]. Neglecting the nonlocal effects, the OEMA provides the Maxwell Garnett approximation and the well-known mixing formulas for the components of the effective permittivity tensor [35]. In Sec. II we write out the effective medium tensors derived in Ref. [31] for the $\mathcal{PT}$-symmetric multilayer in the zeroth, first, and second orders of the OEMA. In Sec. III we discuss the transmission and reflection characteristics and description of $\mathcal{PT}$ symmetry breaking using the local and nonlocal material parameters and find the limits of their applicability. In Sec. IV we generalize the obtained regularities to the two-dimensional $\mathcal{PT}$-symmetric systems. Section V sums up the main results of the article.

II. OPERATOR EFFECTIVE MEDIUM APPROXIMATION FOR A $\mathcal{PT}$-SYMMETRIC MULTILAYER SYSTEM

We consider a $\mathcal{PT}$-symmetric multilayered structure illustrated in Fig. 1. It consists of alternating loss and gain layers of the same thickness $d/2$, the total number of layers being $2N$. To ensure the optical $\mathcal{PT}$ symmetry, the permittivity in the multilayer should be distributed as $\varepsilon(z) = \varepsilon^*(z)$, which is realized using the loss $\varepsilon_L = \varepsilon' + i\varepsilon''$ and gain $\varepsilon_G = \varepsilon' - i\varepsilon''$ permittivities (loss-gain coefficient $\varepsilon'' > 0$). Such a simple structure can be fully described using the transfer-matrix method (TMM), including its transmission and reflection (scattering) properties. We will exploit the TMM for homogenized slabs as well.

To homogenize the multilayered system, we use a recently developed operator effective medium approximation [29,31].

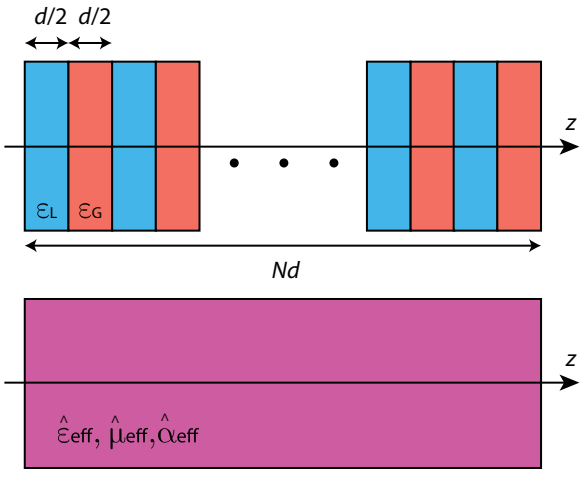

FIG. 1. Geometry of the $\mathcal{PT}$-symmetric system as an N-unit-cell multilayer composed of alternating loss and gain slabs of equal thickness $d/2$ and permittivities $\varepsilon_L = \varepsilon' + i\varepsilon''$ and $\varepsilon_G = \varepsilon' - i\varepsilon''$, respectively. A homogeneous bianisotropic slab with material tensors $\hat{\varepsilon}_{\text{eff}}$, $\hat{\mu}_{\text{eff}}$, and $\hat{\alpha}_{\text{eff}}$ calculated using the OEMA is shown in the bottom part of the sketch.

The idea behind the OEMA is based on writing the fundamental solution for the layered periodic structure as a series over the size parameter $k_0 d$, where k_0 is the vacuum wave number and d is the thickness of the unit cell. Then one is able to introduce the mth order of approximation as a solution containing the terms up to $(k_0 d)^m$. The larger the order, the better the approximation. We do not derive equations for the effective material parameters here, but just borrow them from previous research [31]. Let us start with the zeroth-order ($m = 0$) approximation known as the Maxwell Garnett approximation.

A. Maxwell Garnett approximation

The Maxwell Garnett approach is believed to be valid, if $k_0 d \ll 1$. In this case, the loss-gain multilayer can be represented as a homogeneous uniaxial medium characterized by the permittivity tensor

$$\hat{\varepsilon}^{(0)} = \begin{pmatrix} \varepsilon_{||}^{(0)} & 0 & 0 \\ 0 & \varepsilon_{||}^{(0)} & 0 \\ 0 & 0 & \varepsilon_{\perp}^{(0)} \end{pmatrix},$$
$$\varepsilon_{||}^{(0)} = \frac{\varepsilon_L d/2 + \varepsilon_G d/2}{d} = \varepsilon',$$
$$\varepsilon_{\perp}^{(0)} = \frac{d}{\varepsilon_L^{-1} d/2 + \varepsilon_G^{-1} d/2} = \frac{\varepsilon'^2 + \varepsilon''^2}{\varepsilon'}. \quad (1)$$

Since the size parameter enters the above expression as $(k_0 d)^0$, the Maxwell Garnett approach is the zeroth-order approximation. It should be stressed that this oversimplified technique may not be satisfactory, even if $k_0 d \ll 1$ (see the work on the breakdown of the effective medium theory, e.g., Refs. [36,37]).

B. First-order OEMA

Material parameters in the first-order approximation imply nonlocality and bianisotropy. Bianisotropic (magnetoelectric) terms emerge in the first order, $(k_0 d)^1$, together with the permittivity tensor (1). The magnetoelectric coupling tensor was derived in Ref. [31] and for the loss-gain multilayered system equals

$$\hat{\alpha} = \begin{pmatrix} 0 & \alpha_1 & 0 \\ \alpha_2 & 0 & 0 \\ 0 & 0 & 0 \end{pmatrix}, \quad \alpha_1 = \frac{\varepsilon'' k_0 d}{4},$$
$$\alpha_2 = \frac{\varepsilon'' k_0 d}{4} \left[\frac{2\varepsilon' k_t^2}{k_0^2 (\varepsilon'^2 + \varepsilon''^2)} - 1 \right]. \quad (2)$$

Here the nonlocality appears as evidenced by the dependence of the material parameters on the tangential wave number k_t, i.e., the projection of the wave vector on the interface between slabs. The constitutive equations for such a bianisotropic medium read $\mathbf{D} = \hat{\varepsilon}^{(0)}\mathbf{E} + \hat{\alpha}\mathbf{H}$ and $\mathbf{B} = \mathbf{H} + \hat{\alpha}^T\mathbf{E}$, where $\mathbf{E}$ and $\mathbf{H}$ ($\mathbf{D}$ and $\mathbf{B}$) are the electric and magnetic field strengths (inductions) and superscript T stands for the transposition. It is worth noticing that the magnetoelectric coupling (2) depends on the wave propagation direction, that is, the order of layers ($\varepsilon_L \leftrightarrow \varepsilon_G$ is equivalent to $\varepsilon'' \leftrightarrow -\varepsilon''$).

C. Second-order OEMA

The second-order corrections influence the effective permittivity and permeability tensors keeping the effective magnetoelectric coupling tensors as defined according to Eq. (2). According to Ref. [31], the permittivity and permeability tensors for the loss-gain multilayer take the form

$$\hat{\varepsilon}^{(2)} = \begin{pmatrix} \varepsilon_{||}^{(2)} & 0 & 0 \\ 0 & \varepsilon_{||}^{(2)} & 0 \\ 0 & 0 & \varepsilon_{\perp}^{(2)} \end{pmatrix}, \quad \hat{\mu}^{(2)} = \begin{pmatrix} \mu_{||}^{(2)} & 0 & 0 \\ 0 & \mu_{||}^{(2)} & 0 \\ 0 & 0 & \mu_{\perp}^{(2)} \end{pmatrix},$$

$$\varepsilon_{||}^{(2)} = \varepsilon_{||}^{(0)}(1+w), \quad \varepsilon_{\perp}^{(2)} = \varepsilon_{\perp}^{(0)}(1-w),$$

$$\mu_{||}^{(2)} = 1, \quad \mu_{\perp}^{(2)} = 1 - \frac{(k_0 d)^2}{6} \frac{\varepsilon' \varepsilon''^2}{\varepsilon'^2 + \varepsilon''^2},$$

$$w = \frac{(k_0 d)^2 \varepsilon''^2}{12 \varepsilon'^2} \left[\frac{2\varepsilon' k_t^2}{k_0^2 (\varepsilon'^2 + \varepsilon''^2)} - 1 \right]. \tag{3}$$

The permittivity correction is electric quadrupolar and nonlocal (k_t-dependent). The permeability is caused by the artificial magnetic moment due to the displacement currents. The effective medium in the second-order OEMA is characterized by the constitutive equations $\mathbf{D} = \hat{\varepsilon}^{(2)}\mathbf{E} + \hat{\alpha}\mathbf{H}$ and $\mathbf{B} = \mu^{(2)}\mathbf{H} + \hat{\alpha}^T\mathbf{E}$.

Homogenized PT-symmetric systems are characterized by the peculiar material parameters. They are real-valued quantities, while the permittivity and permeability tensors do not depend on the sign of ε''. Next we will study whether the homogenization is able to predict the positions of exceptional points in $\mathcal{PT}$-symmetric structures.

III. WAVE PROPAGATION IN HOMOGENIZED $\mathcal{PT}$-SYMMETRIC SLAB

A. Normal incidence

Here we compare the scattering properties of homogenized versus multilayered $\mathcal{PT}$-symmetric media. Strictly speaking, the homogenized slab cannot be treated as the $\mathcal{PT}$-symmetric system, but a wave propagation in both systems can be quite similar. Homogenized material is considered as anisotropic (Maxwell Garnett approximation) or nonlocal bianisotropic (first and second order of OEMA) media. In Fig. 2 we demonstrate the transmission T of a normally incident plane wave. In the zeroth-order OEMA, the transmission of the normally incident wave is defined by the in-plane permittivity $\varepsilon_{||}^{(0)}$, which is why it does not depend on the imaginary part of permittivity ε'' [see the horizontal straight line in Fig. 2(a)]. It should be noticed that the Maxwell Garnett approach reproduces the correct value of T only for small ε'', when the second-order corrections are negligible. The region of validity of the first-order OEMA is wider, but it is very limited. In the second order, the transmission spectra will follow the curve corresponding to the transmission through the multilayer. However, this approximation is valid only for the thin unit cells like $d = 100$ nm $\ll \lambda$. For instance, when we double the thickness of the unit cell, the second-order OEMA only qualitatively describes the transmission reproducing peaks but not their positions and heights [see Fig. 2(b)].

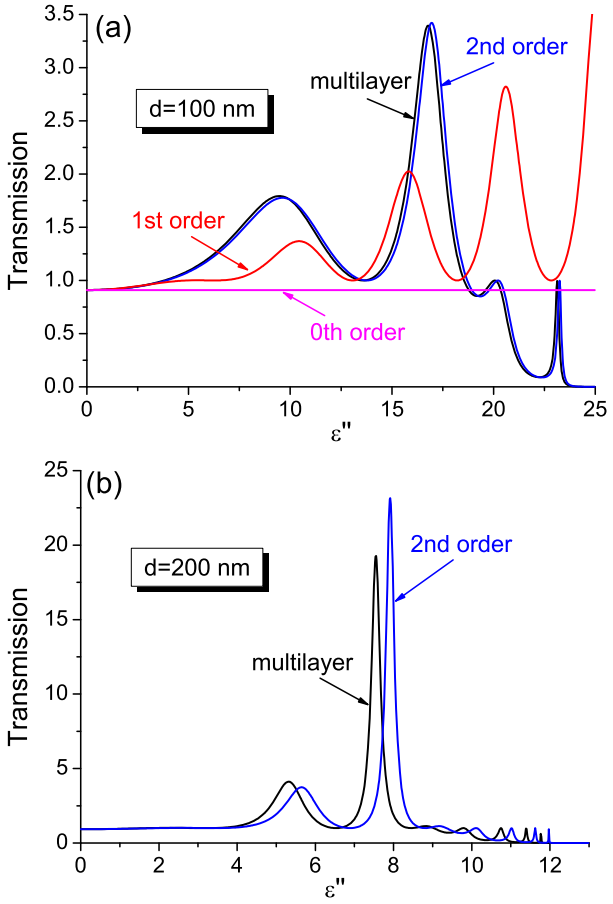

FIG. 2. Transmission of the $\mathcal{PT}$-symmetric multilayer as a function of ε'' calculated within the full TMM (indicated with "multilayer") and OEMA of different orders for the period thickness (a) $d = 100$ nm and (b) $d = 200$ nm. The case of a normally incident wave with $\lambda = 1.55\ \mu$m is considered; the structure consists of $N = 20$ slabs; $\varepsilon' = 2$.

Since the thicknesses of the layers are limited by the validity of the effective medium theory, the large values of the loss-gain coefficient ε'' should be used for reproducing the symmetry breaking in $\mathcal{PT}$-symmetric systems, when loss and gain are no longer balanced. We exploit the standard means for studying the $\mathcal{PT}$ symmetry breakdown, i.e., the calculation of eigenvalues and eigenvectors of the system's scattering matrix. The scattering matrix for the multilayered system and the homogenized medium under consideration can be derived from the corresponding transfer matrix [38]. The eigenvalues of the scattering matrix are unitary ($|s_1| = |s_2| = 1$) in the $\mathcal{PT}$-symmetric state and inverse ($|s_1| = 1/|s_2| > 1$) in the $\mathcal{PT}$-broken state. The eigenvectors of the scattering matrix coalesce at the exceptional point (point of the non-Hermitian singularity), where a phase transition from the $\mathcal{PT}$-symmetric to the non-PT-symmetric state occurs.

Let us examine whether the local or nonlocal homogenization is able to catch the exceptional points of the $\mathcal{PT}$ symmetry breaking. Scattering matrix, transmission, and reflection are expected to be simultaneously well predicted, since the scattering matrix is defined in terms of the amplitude transmission and reflection coefficients. In Fig. 3(a) we show

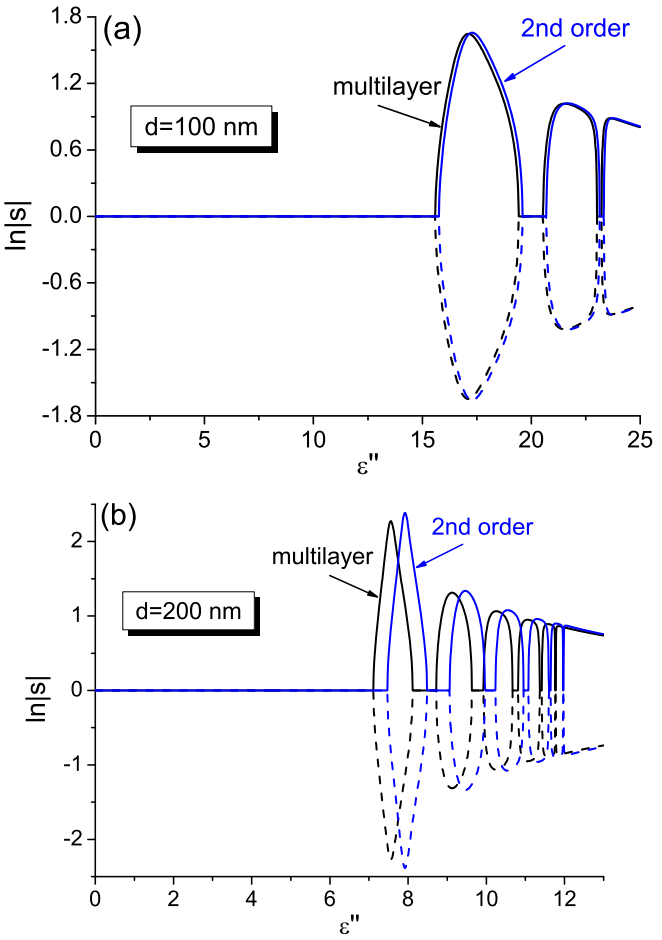

FIG. 3. Dependence of the scattering-matrix eigenvalues on ε'' calculated within the full TMM (indicated by "multilayer") and OEMA of different orders for the period thickness (a) $d = 100$ nm and (b) $d = 200$ nm. Other parameters are the same as in Fig. 2. The first and the second eigenvalues are designated with solid and dashed curves, respectively.

dependence of the eigenvalues of the scattering matrix on ε'' for $d = 100$ nm. Similar to the transmission curves reported in Fig. 2(a), the second-order OEMA correctly describes behavior of the eigenvalues and reproduces the breaking of the $\mathcal{PT}$ symmetry observed in the TMM calculations of the multilayer. The second-order OEMA is also well suited for describing the coalescence of the eigenvectors (not shown here).

Detailed analysis shows that neither the first-order nor zeroth-order OEMA gives a hint of the phase transition. The range of applicability for the Maxwell Garnett approximation is limited by the small loss-gain coefficients ε'', where the $\mathcal{PT}$ symmetry breaking does not occur. The symmetry breaking could be reached for smaller ε'' if the unit cells were thicker. However, the larger d would also ruin the Maxwell Garnett approximation. It is worth mentioning that the homogeneous slab characterized by the permittivity tensor Eq. (1) is inherently inappropriate for description of the exceptional points, because its transmission and reflection properties do not depend on the direction of wave incidence. For instance, in the case of the normal incidence, the properties of the

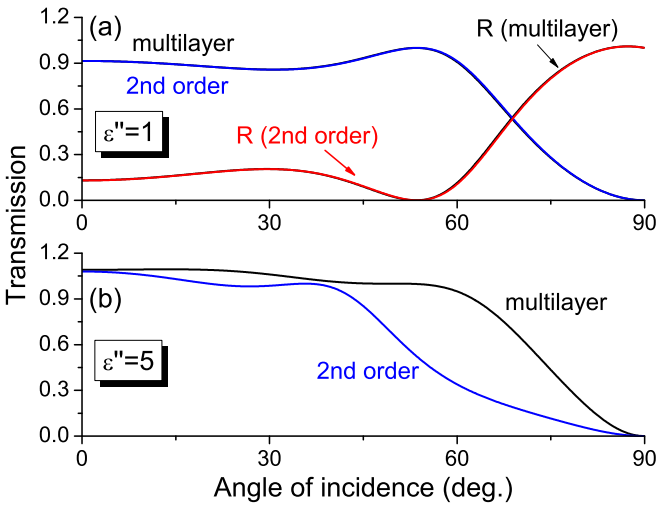

FIG. 4. Angular dependence of transmission for the $\mathcal{PT}$-symmetric multilayer calculated within the full TMM (indicated by "multilayer") and the second-order OEMA. Upper panel shows the results for $\varepsilon'' = 1$, lower panel, for $\varepsilon'' = 5$. Behavior of reflection is shown only for $\varepsilon'' = 1$ and is omitted in the lower panel not to encumber the figure. The period thickness is $d = 100$ nm, and the other parameters are the same as in Fig. 2.

homogeneous slab are equivalent to those of an isotropic dielectric slab of permittivity ε'.

The breakdown of the $\mathcal{PT}$ symmetry cannot be also obtained if we skip the terms proportional to $(k_0 d)^1$ and leave the second-order terms $(k_0 d)^2$. This means that only the mix of the first-order and second-order terms properly reproduces the eigenvalues. As previously, the thicker layers ruin the correspondence between the exact and homogenized description of the structure [Fig. 3(b)]. The difference between the accurate and approximate eigenvalues is mainly the shift along the ε'' axis. The eigenvalues in the second-order OEMA $s^{(2)}$ are roughly related to the eigenvalues of the $\mathcal{PT}$-symmetric multilayer s as $s(\varepsilon'') \approx s^{(2)}(\varepsilon'' + ak_0 d)$, where the shift is proportional to the size parameter $k_0 d$ and a is a constant. Hence, we can estimate the higher-order corrections caused by excitation of the higher-order multipoles as $[ds^{(2)}(\varepsilon'')/d\varepsilon'']ak_0 d$.

B. Oblique incidence

Now we face the dependence of the multilayer response on the incidence angle of the plane waves. In Fig. 4 we observe a strong dependence of the correctness of the homogenization on the value of ε''. For $\varepsilon'' = 1$, both transmission and reflection dependencies on the incidence angle are reliably described by the second-order OEMA, but this is not already the case at $\varepsilon'' = 5$. This discrepancy grows with the increase of ε'': the second-order OEMA may even predict a number of artifact peaks absent in the curves calculated for the multilayer.

The validity of the nonlocal effective medium approximation of the second order is determined by the loss-gain coefficient ε'' but not the angle of incidence. We relate the behavior shown in Fig. 4(b) to the appearance of the $\mathcal{PT}$-symmetry-broken states for the larger incidence angles. At the oblique incidence, the light passes a longer path compared to

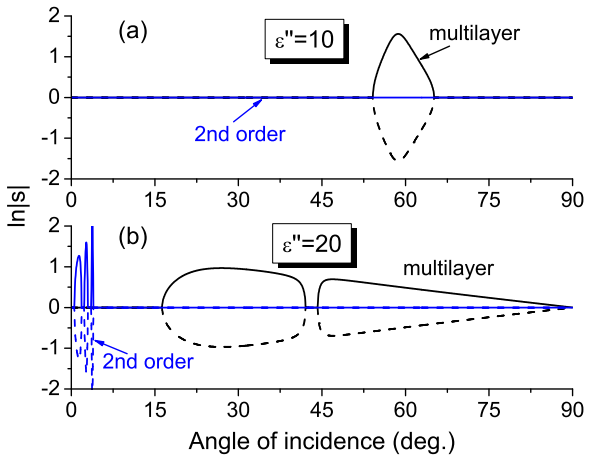

FIG. 5. Angular dependence of the scattering-matrix eigenvalues calculated within the full TMM (indicated by "multilayer") and the second-order OEMA. The upper panel shows the results for $\varepsilon'' = 10$, the lower one, $\varepsilon'' = 20$. The other parameters are the same as in Fig. 4. The first and the second eigenvalues are designated with solid and dashed curves, respectively.

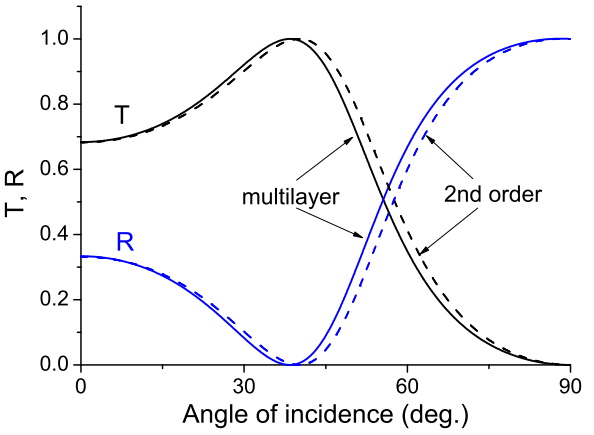

FIG. 6. Angular dependence of transmission and reflection calculated within the full TMM (indicated by "multilayer") and the second-order OEMA for $\varepsilon' = 10$ and $\varepsilon'' = 1$. The other parameters are the same as in Fig. 4.

the normal incidence; therefore, the effective thickness of the structure is enlarged, and exceptional points of the $\mathcal{PT}$ symmetry breaking may appear at the smaller ε''. In Fig. 5 we plot the angular dependencies of the scattering matrix eigenvalues for $\varepsilon'' = 10$ and $\varepsilon'' = 20$. The results for the multilayered and homogenized structures are qualitatively different in these cases. The OEMA cannot catch the $\mathcal{PT}$-symmetry-broken state for $\varepsilon'' = 10$, because it does not properly enlarge the effective thickness at the oblique incidence. Indeed, the effect of the tangential wave number k_t is negligible for the great ε'' [see Eqs. (2) and (3)]; i.e., the results are quite close to those for $k_t = 0$. As well as for the normal incidence, the $\mathcal{PT}$-symmetry-broken states appear at the larger $\varepsilon'' = 20$, but they do not correspond to the accurate calculations.

According to Eqs. (2) and (3), the wave number k_t makes significant effect for the greater real part of the permittivity ε'. Figure 6 shows the angular dependencies of transmission and reflection at $\varepsilon' = 10$ and small loss-gain coefficient $\varepsilon'' = 1$. Comparing with the good matching of the accurate and approximate results for $\varepsilon' = 2$ and $\varepsilon'' = 1$ (see Fig. 4), one can note that there is some discrepancy between the OEMA and accurate calculations, but only in the region of large incidence angles. We conclude that the nonlocal homogenization may be applicable if ε'' is not much greater than ε'.

IV. HOMOGENIZATION OF TWO-DIMENSIONAL $\mathcal{PT}$-SYMMETRIC SYSTEMS

Although we have considered only one-dimensional structures above, two-dimensional $\mathcal{PT}$-symmetric systems also can be homogenized. Two-dimensional $\mathcal{PT}$ symmetry can be introduced in a system of periodically arranged z-oriented waveguides as in Ref. [39]. The system of waveguides can be nonlocally homogenized in different ways. In concordance with a coherent-potential approximation [40–42], a unit cell of the periodic array should not scatter light if it is embedded into a proper effective medium. Such a condition can be easily written for a single cylinder, but it is much more complicated for the unit cell in Fig. 7 (loss and gain waveguides of the same radius r in the cell). Nevertheless, the effective material parameters in the limit of small cylinder radii $k_0 r \ll 1$ should have a similar form for the single cylinder and four cylinders in the cell. Thus, in the case of the two-dimensional $\mathcal{PT}$-symmetric structure one writes $\hat{\varepsilon} = \mathrm{diag}(\varepsilon_x, \varepsilon_y, \varepsilon_z)$, where [42]

$$\varepsilon_x = \varepsilon_y = \varepsilon_x^{(0)}, \quad \varepsilon_z = \frac{\varepsilon_z^{(0)} + \alpha\rho(\varepsilon_L + \varepsilon_G)k_z^2}{1 + 2\alpha\rho k_z^2}. \tag{4}$$

Here α is the parameter defined by the cell geometry, and ρ is the filling factor of loss (gain) material. The Maxwell Garnett permittivities are equal to

$$\varepsilon_x^{(0)} = \rho(\varepsilon_L + \varepsilon_G) + (1 - 2\rho)\varepsilon_h,$$
$$\varepsilon_z^{(0)} = \varepsilon_h \frac{1+p}{1-p}, \quad p = 2\rho \frac{\varepsilon_L\varepsilon_G - \varepsilon_h^2}{(\varepsilon_L + \varepsilon_h)(\varepsilon_G + \varepsilon_h)}, \tag{5}$$

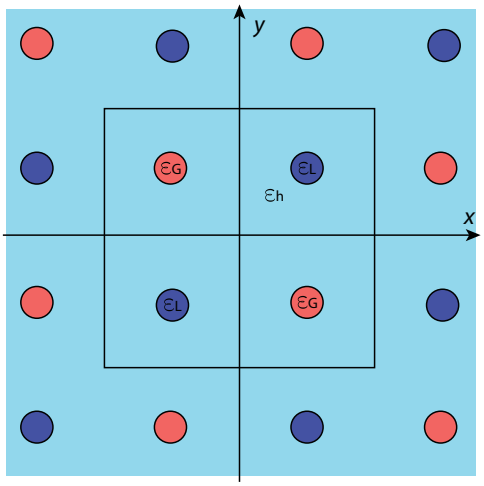

FIG. 7. Square unit cell of the two-dimensional $\mathcal{PT}$-symmetric structure comprising four z-oriented circular waveguides.

where ε_h is the host medium permittivity.

The nonlocal permittivity ε_z in Eq. (4) depends on the wave number k_z. It is obtained as a series expansion of the zeroth Mie coefficient for TM-polarized waves [42]. This means that the nonlocality is related to the toroidal moment [43], but not to the quadrupole moment defined by the second Mie coefficient [44]. On the other hand, as we have discussed above, the electric quadrupole moment is needed for predicting exceptional points in $\mathcal{PT}$-symmetric multilayers. Thus, the homogenization carried out using the coherent-potential approximation cannot reproduce exceptional points of $\mathcal{PT}$ symmetry breaking as well as the Maxwell Garnett approximation.

Another approach is the nonlocal homogenization theory, which can be applied to an arbitrary metamaterial. The effective dielectric permittivity tensor of the homogenized medium takes the form [30]

$$\varepsilon_{ij}^{(2)} = \varepsilon_{ij} + i\alpha_{ijr}k_r - \beta_{ijrs}k_r k_s, \tag{6}$$

where the summation over repeated indices is employed, indices i, j, r, and s run from 1 to 3, and k_r is the r-component of the wave vector. Tensors in Eq. (6) depend on distribution of the permittivity in the metamaterial $\varepsilon(\mathbf{r}) = \varepsilon'(\mathbf{r}) + i\varepsilon''(\mathbf{r})$ and expansion parameter $k_0 d$, being symmetric $\varepsilon_{ij} = \varepsilon_{ji} = \xi_{ij}^{(1)} + (k_0 d)^2 \xi_{ij}^{(2)}$, $\beta_{ijrs} = \beta_{jirs} = (k_0 d)^2 \gamma_{ijrs}$ or antisymmetric $\alpha_{ijr} = -\alpha_{jir} = (k_0 d)\zeta_{ijr}$. The condition for $\mathcal{PT}$ symmetry $\varepsilon(\mathbf{r}) = \varepsilon^*(-\mathbf{r})$ imposes the following restrictions on the tensors: $\varepsilon_{ij} = \varepsilon_{ij}^*$, $\alpha_{ijr} = -\alpha_{ijr}^*$, and $\beta_{ijrs} = \beta_{ijrs}^*$. The Maxwell Garnett approximation corresponds to $\varepsilon_{ij}^{(0)} = \xi_{ij}^{(1)}$. The structure of Eq. (6) is similar to that of the periodic multilayer. In both approaches, the zeroth order corresponds to the Maxwell Garnett approximation, the first order introduces gyrotropy (chirality), and the second order takes into account quadrupole moment. Moreover, in Ref. [30] the general nonlocal homogenization theory was applied for the stack of layers. Therefore, Eq. (6) is an ansatz for both one- and two-dimensional $\mathcal{PT}$-symmetric systems, and, hence, prediction of the exceptional points should be valid in the general case. Homogenization of two-dimensional $\mathcal{PT}$-symmetric systems in detail deserves separate investigation.

V. CONCLUSION

To conclude, we have studied the local and nonlocal homogenization of the $\mathcal{PT}$-symmetric multilayered system. It has been carried out using the previously developed operator effective medium approximation providing the successive approximations for effective parameters including the usual mixing (Maxwell Garnett) formulas and the nonlocal bianisotropic material tensors. We have found that the Maxwell Garnett approach is entirely inappropriate for description of the $\mathcal{PT}$ symmetry. The nonlocal model takes into account the distribution of the loss and gain materials and can be applied in the limit of electrodynamically small thicknesses of the unit cells. Such behavior is equally related to the transmission and scattering matrix eigenvalues spectra. For the obliquely incident plane waves, the validity of the nonlocal homogenization is limited by the loss-gain coefficients ε'' comparable to or smaller than the real part of the permittivity ε'. Thus, though the nonlocal homogenization is applicable, it is strongly restricted by the thickness of the unit cell and the value of the loss-gain coefficient.

ACKNOWLEDGMENTS

The work was supported by the Belarusian Republican Foundation for Fundamental Research (Project No. F18R-021), the Russian Foundation for Basic Research (Projects No. 18-02-00414, No. 18-52-00005, and No. 18-32-00160), the Ministry of Education and Science of the Russian Federation (GOSZADANIE, Grant No. 3.4982.2017/6.7), and the Government of the Russian Federation (Grant No. 08-08). Calculations of transmission and reflection from periodic media were supported by the Russian Science Foundation (Project No. 17-72-10098).

[1] C. M. Bender and S. Boettcher, Phys. Rev. Lett. **80**, 5243 (1998).
[2] C. M. Bender, Rep. Prog. Phys. **70**, 947 (2007).
[3] R. El-Ganainy, K. G. Makris, D. N. Christodoulides, and Z. H. Musslimani, Opt. Lett. **32**, 2632 (2007).
[4] C. E. Rüter, K. G. Makris, R. El-Ganainy, D. N. Christodoulides, M. Segev, and D. Kip, Nat. Phys. **6**, 192 (2010).
[5] Y. Liu, T. Hao, W. Li, J. Capmany, N. Zhu, and M. Li, Light Sci. Appl. **7**, 38 (2018).
[6] L. Feng, R. El-Ganainy, and L. Ge, Nat. Photon. **11**, 752 (2017).
[7] R. El-Ganainy, K. G. Makris, M. Khajavikhan, Z. H. Musslimani, S. Rotter, and D. N. Christodoulides, Nat. Phys. **14**, 11 (2018).
[8] D. V. Novitsky, A. Karabchevsky, A. V. Lavrinenko, A. S. Shalin, and A. V. Novitsky, Phys. Rev. B **98**, 125102 (2018).
[9] L. Feng, Z. J. Wong, R.-M. Ma, Y. Wang, and X. Zhang, Science **346**, 972 (2014).
[10] H. Hodaei, M.-A. Miri, M. Heinrich, D. N. Christodoulides, and M. Khajavikhan, Science **346**, 975 (2014).
[11] S. Longhi, Phys. Rev. A **82**, 031801(R) (2010).
[12] Z. J. Wong, Y.-L. Xu, J. Kim, K. O'Brien, Y. Wang, L. Feng, and X. Zhang, Nat. Photon. **10**, 796 (2016).
[13] W. Chen, S. K. Özdemir, G. Zhao, J. Wiersig, and L. Yang, Nature (London) **548**, 192 (2017).
[14] H. Hodaei, A. U. Hassan, S. Wittek, H. Garcia-Gracia, R. El-Ganainy, D. N. Christodoulides, and M. Khajavikhan, Nature (London) **548**, 187 (2017).
[15] P.-Y. Chen, M. Sakhdari, M. Hajizadegan, Q. Cui, M. M.-C. Cheng, R. El-Ganainy, and A. Alù, Nat. Electron. **1**, 297 (2018).
[16] Z. Lin, H. Ramezani, T. Eichelkraut, T. Kottos, H. Cao, and D. N. Christodoulides, Phys. Rev. Lett. **106**, 213901 (2011).
[17] K. G. Makris, R. El-Ganainy, D. N. Christodoulides, and Z. H. Musslimani, Phys. Rev. Lett. **100**, 103904 (2008).
[18] K. Ji, Z. Wen, Z. Liu, Y. Dai, K. Han, P. Gao, A. Gao, J. Bai, G. Zhang, and X. Qi, Opt. Lett. **43**, 4457 (2018).
[19] R. Fleury, D. L. Sounas, and A. Alù, Phys. Rev. Lett. **113**, 023903 (2014).
[20] M. Lawrence, N. Xu, X. Zhang, L. Cong, J. Han, W. Zhang, and S. Zhang, Phys. Rev. Lett. **113**, 093901 (2014).

[21] M. Sarisaman and M. Tas, J. Opt. Soc. Am. B **35**, 2423 (2018).
[22] A. Guo, G. J. Salamo, D. Duchesne, R. Morandotti, M. Volatier-Ravat, V. Aimez, G. A. Siviloglou, and D. N. Christodoulides, Phys. Rev. Lett. **103**, 093902 (2009).
[23] L. Feng, Y.-L. Xu, W. S. Fegadolli, M.-H. Lu, J. E. B. Oliveira, V. R. Almeida, Y.-F. Chen, and A. Scherer, Nat. Mater. **12**, 108 (2013).
[24] A. S. Shalin, P. Ginzburg, A. A. Orlov, I. Iorsh, P. A. Belov, Yu. S. Kivshar, and A. V. Zayats, Phys. Rev. B **91**, 125426 (2015).
[25] A. V. Chebykin, A. A. Orlov, A. S. Shalin, A. N. Poddubny, and P. A. Belov, Phys. Rev. B **91**, 205126 (2015).
[26] A. P. Slobozhanyuk, P. Ginzburg, D. A. Powell, I. Iorsh, A. S. Shalin, P. Segovia, A. V. Krasavin, G. A. Wurtz, V. A. Podolskiy, P. A. Belov, and A. V. Zayats, Phys. Rev. B **92**, 195127 (2015)
[27] A. Alù, Phys. Rev. B **84**, 075153 (2011).
[28] A. V. Novitsky, V. M. Galynsky, and S. V. Zhukovsky, Phys. Rev. B **86**, 075138 (2012).
[29] Y. Liu, S. Guenneau, and B. Gralak, Proc. R. Soc. A **469**, 20130240 (2013).
[30] A. Ciattoni and C. Rizza, Phys. Rev. B **91**, 184207 (2015).
[31] V. Popov, A. V. Lavrinenko, and A. Novitsky, Phys. Rev. B **94**, 085428 (2016).
[32] I. Tsukerman, J. Opt. Soc. Am. B **28**, 577 (2011).
[33] O. V. Shramkova and G. P. Tsironis, Phys. Rev. B **94**, 035141 (2016).
[34] V. Popov, A. V. Lavrinenko, and A. Novitsky, Phys. Rev. B **97**, 125428 (2018).
[35] V. A. Markel, J. Opt. Soc. Am. A **33**, 1244 (2016).
[36] H. Herzig Sheinfux, I. Kaminer, Y. Plotnik, G. Bartal, and M. Segev, Phys. Rev. Lett. **113**, 243901 (2014).
[37] S. V. Zhukovsky, A. Andryieuski, O. Takayama, E. Shkondin, R. Malureanu, F. Jensen, and A. V. Lavrinenko, Phys. Rev. Lett. **115**, 177402 (2015).
[38] L. Ge, Y. D. Chong, and A. D. Stone, Phys. Rev. A **85**, 023802 (2012).
[39] M. Kremer, T. Biesenthal, L. J. Maczewsky, M. Heinrich, R. Thomale, and A. Szameit, Nature Commun. **10**, 435 (2019).
[40] Y. Wu, J. Li, Z.-Q. Zhang, and C. T. Chan, Phys. Rev. B **74**, 085111 (2006).
[41] B. A. Slovick, Z. G. Yu, and S. Krishnamurthy, Phys. Rev. B **89**, 155118 (2014).
[42] T. Geng, S. Zhuang, J. Gao, and X. Yang, Phys. Rev. B **91**, 245128 (2015).
[43] W. Liu, J. Zhang, and A. E. Miroshnichenko, Laser Photon. Rev. **9**, 564 (2015).
[44] A. Novitsky, W. Ding, M. Wang, D. Gao, A. V. Lavrinenko, and C.-W. Qiu, Sci. Rep. **7**, 652 (2017).